Atmospheric Environment 68 (2013) 256–264

Contents lists available at SciVerse ScienceDirect

Atmospheric Environment

journal homepage: www.elsevier.com/locate/atmosenv

Assessing exposure risk for dust storm events-associated lung function decrement in asthmatics and implications for control

Nan-Hung Hsieh, Chung-Min Liao*

Department of Bioenvironmental Systems Engineering, National Taiwan University, Taipei 10617, Taiwan, ROC

HIGHLIGHTS

- Aerosol binding kinetic-based toxicodynamic model can predict dust aerosol induced FEV_1 decrement.
- Probabilistic risk framework can assess dust storm events-induced FEV_1 decrement.
- The surgical mask with activated carbon can control dust storm attack effectively.

ARTICLE INFO

Article history:
Received 15 October 2012
Received in revised form
18 November 2012
Accepted 29 November 2012

Keywords:
Asian dust storm
Asthma
Lung function
Probabilistic risk assessment
Respiratory protection

ABSTRACT

Asian dust storms (ADS) events are seasonally-based meteorological phenomena that exacerbate chronic respiratory diseases. The purpose of this study was to assess human health risk from airborne dust exposure during ADS events in Taiwan. A probabilistic risk assessment framework was developed based on exposure and experimental data to quantify ADS events induced lung function decrement. The study reanalyzed experimental data from aerosol challenge in asthmatic individuals to construct the dose–response relationship between inhaled dust aerosol dose and decreasing percentage of forced expiratory volume in 1 s ($\%FEV_1$). An empirical lung deposition model was used to predict deposition fraction for size specific dust aerosols in pulmonary regions. The toxicokinetic and toxicodynamic models were used to simulate dust aerosols binding kinetics in lung airway in that $\%FEV_1$ change was also predicted. The mask respirators were applied to control the inhaled dose under dust aerosols exposure. Our results found that only 2% probability the mild ADS events were likely to cause $\%FEV_1$ decrement higher than 5%. There were 50% probability of decreasing $\%FEV_1$ exceeding 16.9, 18.9, and 7.1% in north, center, and south Taiwan under severe ADS events, respectively. Our result implicates that the use of activated carbon of mask respirators has the best efficacy for reducing inhaled dust aerosol dose, by which the $\%FEV_1$ decrement can be reduced up to less than 1%.

1. Introduction

Asthma is a chronic respiratory disease (CRD) affecting millions of children and adults worldwide (GINA, 2012). Asthma is mainly caused by airflow obstruction resulting from inflammation and remodeling in the sensitive small airways. The allergic disease can attack abruptly due to constriction of airway in response to environmental stimuli (Venegas et al., 2005; Frey et al., 2011).

Air pollution is the common environmental stimuli included oxidative chemicals and particulate matters (PMs) which are most likely to associate with asthma severity (Lee et al., 2003; Chen et al., 2006; Tsai et al., 2006; Bell et al., 2008). The properties of PMs such as size, surface area and chemical compositions determine the different levels of health effects (Nel, 2005; Pope and Dockery, 2006). The suspension of solid particles with smaller size can penetrate deeper into lung tissue by respiration (ICRP, 1994). The pulmonary effects caused by inhaled particles depend on the location at which they deposit within the respiratory airways (Ruzer and Harley, 2005). In addition, sandstorm dusts generated PMs have strong association with asthma exacerbations and increased cardiopulmonary disease mortality (Chan and Ng, 2011; Hong et al., 2010).

The Asian dust storm (ADS) events are seasonally-based meteorological phenomena. The concentrated clouds of fine, dry sand particles mainly originated in the deserts of Mongolia, northern China and Kazakhstan affect air quality in East Asia, including Taiwan during the springtime (March–May) (Liu et al., 2006). Recent studies demonstrated that dust storm events were associated with asthma

* Corresponding author. Tel.: +886 2 2363 4512; fax: +886 2 2362 6433.
E-mail address: cmliao@ntu.edu.tw (C.-M. Liao).

1352-2310/$ – see front matter © 2012 Elsevier Ltd. All rights reserved.
http://dx.doi.org/10.1016/j.atmosenv.2012.11.064

exacerbations induced respiratory symptoms and lung function disorder (Hong et al., 2010). Dust aerosol is a pro-inflammatory trigger that induces inflammatory response in subjects and contributes to the risk of developing asthma and COPD. Furthermore, dust aerosols in buildings are significantly affected by outdoor air pollutants and may also associated with allergies, asthma, and other respiratory conditions (Kuo and Shen, 2010).

Lung function has been suggested as an excellent operative marker for bronchial hyperreactivity and constriction, providing a useful reference in the chronic airway diseases severity (Weiss, 2010). The laboratory aerosol challenge from Gupta et al. (2012) indicated that sandstorm dust with smaller size could associate with greater potential effects for forced expiratory volume in 1 s (FEV_1) decrement. On assessing the effects of dust storm events on patients with asthma, Hong et al. (2010) found the metal concentrations bounded to dust aerosols were significantly associated with lung function index of peak expiratory flow (PEF) decrement among childhood asthmatics.

The purpose of this study was to construct a quantitative risk assessment framework for assessing the dust storm events attacks for asthmatics. This study reanalyzed published data of size-dependent dust aerosols from an experimental aerosol challenge for patient with asthma. A two-compartment dynamic model was used to estimate the airway binding aerosols-induced lung function decrement appraised with the Asian dust storm data to estimate deposition doses in lung regions based on different exposure scenarios in Taiwan. We also quantified the impact of different face mask interventions on reducing dust aerosols exposure for airway function in asthmatics.

2. Materials and methods

2.1. Study data

This study collected regional-scale data of dust storm events occurred in north, central, and south Taiwan regions represented by Taipei (N-TP), Taichung (C-TC), and Pingtung (S-PT) cities, respectively. The size distributions of ADS aerosols in three regions were also collected. To compare the health impact of dust aerosols in indoor and outdoor environments, this study adopted the previous studies on investigation of the indoor and outdoor airborne PM concentrations for $PM_{2.5}$ and PM_{10} (particles diameter less than 2.5 and 10 μm), respectively, during dust storm periods (Fang et al., 2002; Chen et al., 2004; Lee et al., 2006; Kuo and Shen, 2010). Recent dust storms events were collected to reflect the increasing of climate change-induced serious dust storms events. Based on Taiwan Environmental Protection Admission (EPA, Taiwan) database, the Air Quality Monitoring Network revealed that the highest PM concentration in the year of 2010 dust storm period had the most serious episode in the last 20 years. We also analyzed the monitoring data from regional stations to compare with the past general dust storm events discussed in the previous studies.

The valuable datasets provided by Gupta et al. (2012) give us the unique opportunity to examine the effects of dust aerosols on lung function decreasing in chronic asthmatic subjects. In brief, Gupta et al. (2012) examined the change of FEV_1 for 20 asthmatics with mean age of 26.6 yrs based on the experimental dust aerosol challenge. Four types of size-dependent soil samples included one type of clay soil (C1) and three types of sand soil (S1, S2, and S3) were collected to generate dust cloud in exposure chamber. All experimental dust aerosols are polydisperse. After inhaled the dust aerosols in exposure chamber, values of FEV_1 for asthmatics were measured at 5-, 15-, 30-, and 60-min post challenge. Gupta et al. (2012) found the maximal decline in FEV_1 for four dust samples were occurred in 15 min post challenge, and the mean decline values in FEV_1 were between 0.32 and 0.69 L. The time-course of percent FEV_1 ($\%FEV_1$) decrement was also shown the similar results. They also found that the decline in FEV_1 correlated with volume percentage of dust aerosols with size less than 10 μm. The clay soil had the smallest size distribution given the greatest effect for asthmatics, which can reduce the maximum of $\%FEV_1$ to 20.22%.

2.2. Exposure and effect analysis

To evaluate the exposure risk, we first predicted the amount of particles deposited in the human lung following the exposure to airborne PM. We reconstructed the mass-basis dosimetric exposure model as,

$$D = C \times DF \times ED \times BR, \tag{1}$$

where D is the mass-based cumulative dose of inhaled dust (μg), C is the mass concentration of airborne dust (μg m^{-3}), BR is the breathing rate (0.38 ± 0.07 m^3 h^{-1}) which based on the investigation for Taiwanese (DOH, 2007), ED is the exposure duration (1 h), and DF is the PM deposition fraction in different human lung regions. We reanalyzed the particle size distribution by Monte Carlo (MC) simulation to estimate the size-dependent deposition fraction among different lung regions. The inhaled dust aerosols were also treated probabilistically via MC simulation.

To simulate the inhaled dust aerosols which deposit in different respiratory regions, we adopted the simplified equations that fit to the empirical model for monodisperse spheres with standard density and conditions, based on the International Commission on Radiological Protection (ICRP) deposition model (ICRP, 1994; Hinds, 1999). The models were suited for males and females at different exercise levels. In the size range of 0.001–100 μm, the errors of deposition fractions predicted by these equations agreed with the ICRP model within ±3% (Hinds, 1999).

The deposition fraction for the extrathoracic (ET) region DF_{ET} is

$$DF_{ET} = IF\left(\frac{1}{1+\exp(6.84+1.183\ln d_p)} + \frac{1}{1+\exp(0.924-1.885\ln d_p)}\right), \tag{2}$$

where d_p is particle size (μm) and IF is the inhalable fraction, given by

$$IF = 1 - 0.5\left(1 - \frac{1}{1+0.00076{d_p}^{2.8}}\right). \tag{3}$$

The deposition fraction for the tracheobronchial (TB) region DF_{TB} is

$$DF_{TB} = \left(\frac{0.00352}{d_p}\right)\left[\exp\left(-0.234(\ln d_p+3.40)^2\right) + 63.9\exp\left(-0.189(\ln d_p-1.61)^2\right)\right], \tag{4}$$

and the deposition fraction for the alveolar-interstitial (AI) region DF_{AI} is

$$DF_{AI} = \left(\frac{0.0155}{d_p}\right)\left[\exp\left(-0.416(\ln d_p+2.84)^2\right) + 19.11\exp\left(-0.482(\ln d_p-1.362)^2\right)\right]. \tag{5}$$

To understand the effect of dust aerosol-associated lung function change, we developed a toxicokinetic (TK)/toxicodynamic (TD) model based on the previous studies (Freijer et al., 2002; Amin

et al., 2010). Amin et al. (2010) used a simple, two-compartment pharmacokinetic (PK) model to describe the time course of agonist diffusion and binding in lung airway smooth muscle (ASM) receptors. This model focused on the kinetics of agonist-receptor binding and the resulting airway wall mechanics of restriction. To predict lung function change under dust aerosol exposure, we adopted the TD model from Freijer et al. (2002) which simulate lung function of FEV_1 change under environmental stimuli exposure. Using clinical human studies, this model can predict cellular injury/repair and lung function overtime. The lung function dynamics in their model were based on the epithelial cell coverage percentage. Therefore, the TK/TD of lung function effect due to PM exposure scenario can be constructed.

We linked previous developed TK and TD models to simulate plausible effect under dust aerosols exposure. The model parameters for aerosols binding kinetics were based on the values from Amin et al. (2010). The present TK/TD model not only predicts the kinetics of binding dose in ASM receptors but also simulates time course of lung function changes. The dynamics of ordinary differential equations corresponding to the TK/TD model (Fig. 1) can be expressed as,

$$\frac{dD_W(t)}{dt} = -k_b D_W(t) + k_u D_R(t) - cD_W(t), \tag{6}$$

$$\frac{dD_R(t)}{dt} = k_b D_W(t) - k_u D_R(t), \tag{7}$$

$$\frac{dF(t)}{dt} = \lambda_1 D_R(t) - \lambda_2 F(t), \tag{8}$$

where D_W and D_R are the inhaled dose of the dust aerosols in the airway wall tissue and airway smooth muscle receptors (μg), respectively, F is the percentage decrease for FEV_1 comparing with non-exposure scenario, t is the time (min), k_b and k_u are the binding and unbinding rates for the compartments of airway wall tissue and smooth muscle receptors (min^{-1}), respectively, c is the clearance rate (min^{-1}), λ_1 is the sensitization rate (μg min^{-1}), and λ_2 is the desensitization rate (min^{-1}).

This study used the deposition dust aerosols in TB region as the initial condition of the inhaled dose in airway wall tissue due to that ASM was contained in bronchial branches. The bronchus is also an important compartment of the respiratory system which can reflect the airway constriction in lung function.

We constructed the dose–response profile by fitting nonlinear Hill model to the predicted values on binding aerosols that cause adverse effects as

$$R(D) = \frac{R_{max} \cdot D^n}{R50^n + D^n}, \tag{9}$$

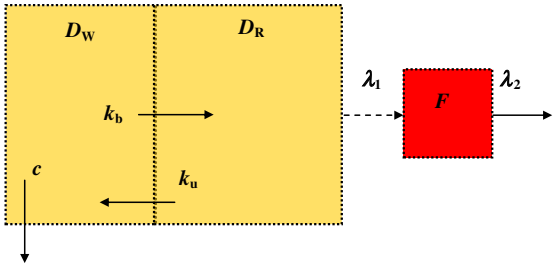

Fig. 1. Block diagram of the TK/TD model for aerosols binding kinetics and lung function changes.

where D is the cumulative dust aerosol dose, R_{max} is the maximum predicted response where we used $\%FEV_1$ decrement for asthmatics, $R(D)$ is the response for the specific binding dose of dust aerosols, $R50$ represents the dose that causes half maximum response, and the exponent n is the fitted Hill coefficient.

2.3. Probabilistic risk model

Risk characterization is the phase of risk assessment where the results of the dust aerosols are associated with a quantitative effect on asthma severity. The risk at a specific inhaled dose for dust aerosol can be calculated as the probability density function (pdf) of the ASM binding aerosol dose multiplied by the conditional probability of lung function effect with given ASM binding dose in receptors. In this study, probabilistic risk model was used to characterize the lung function decrement risk for asthmatics posed by dust aerosols. A joint probability function (JPF) can be used to calculate the risk probability as,

$$P(R_F) = P(D_R) \times P(R_F|D_R), \tag{10}$$

where $P(R_F)$ represents the risk of $\%FEV_1$ decrement for asthmatics, $P(D_R)$ is the pdf of internal binding dose of dust aerosols and $P(R_F|D_R)$ is the conditional probability of the adverse effect given the specific internal binding dose in receptors. Here, $P(R_F|D_R)$ can be considered as a Hill-based dose–response function in Eq. (10).

A risk profile was generated from the cumulative distribution of simulation outcomes. Each point on the risk curve represents the probability that the lung function will exacerbate to the higher level. The x-axis of the risk curve can be interpreted as a magnitude of lung function effect and y-axis can be interpreted as the probability that an exacerbation effect of at least that magnitude will occur.

2.4. Health protective strategy

The respiration protectors were considered as the health protective strategy in reducing dust aerosols exposure. This study adopted the filtration efficiency of surgical mask to quantify the control impact on the health care effect. Chen (2001) examined the different types of mask which were widely sold in Taiwan markets. The compositions of masks included: non-woven material only (general mask) and non-woven material combined with activated carbon fiber (activated carbon mask). The filtration efficiency of masks was dependent on the size of solid particles. The filtration efficiencies of general mask and activated carbon mask ranged from 20 to 60% and 55% to 90% for 0.1–1 μm of challenge particles, respectively. Under this size range, the filtrated mechanisms of the mask included impaction, diffusion and interception. The derived model from challenge particles can be used to predict the dust-mask filtration performances. We can simulate the uncontrollable inhaled dust aerosol dose by considering the filtration efficiency of different masks. The exposure risk with control measures of general mask and activated carbon mask were further assessed.

2.5. Uncertainty and data analysis

To understand the best fitted parameters for study data, we applied TableCurve 2D (AISN Software Inc., Mapleton, OR, USA) to judge the optimal statistical model selected based on the least-square criterion from a set of linear and nonlinear models. Simulations of the TK/TD model were performed by using ode45 solver in Berkley Madonna: Modeling and Analysis of Dynamic Systems (Version 8.3.9, Berkley Madonna Inc). In exposure and risk assessment, there have several sources of uncertainty. A MC simulation was implemented to quantify the uncertainty and its impact on the

estimation of expected risk by Crystal Ball® software (Version 2000.2, Decisionerring, Inc., Denver, CO, USA) which carried out with 10,000 iterations to assure the stability of those pdfs and generate 2.5- and 97.5-percentiles as the 95% confidence interval (CI) for all fitted models.

3. Results

3.1. Dose–response assessment

Fig. 2A shows the reconstructed fraction of airborne dust size distributions for challenge aerosols in asthmatic subjects (Gupta et al., 2012). The simulation provided adequate descriptions to characterize the physical properties for all dust aerosols from experimental data. The log-normal distribution can best describe the size distribution of four types of dust aerosols represented as LN(geometric mean (gs), geometric standard deviation (gsd)). The size distributions for clay (C1) and sand (S1, S2, and S3) dusts were LN(0.4 μm, 2.9), LN(2.7 μm, 2.3), LN(7.1 μm, 1.9), and LN(8.1 μm, 1.8) respectively, indicating that clay dust had smaller particle size with larger dispersion than sand dusts. We also found that the clay dust had the smallest mass median diameter (MMD) of nearly 11 μm.

Fig. 2B–G shows the deposition fraction of dust aerosols in different lung regions calculated by the ICRP model. The ET region

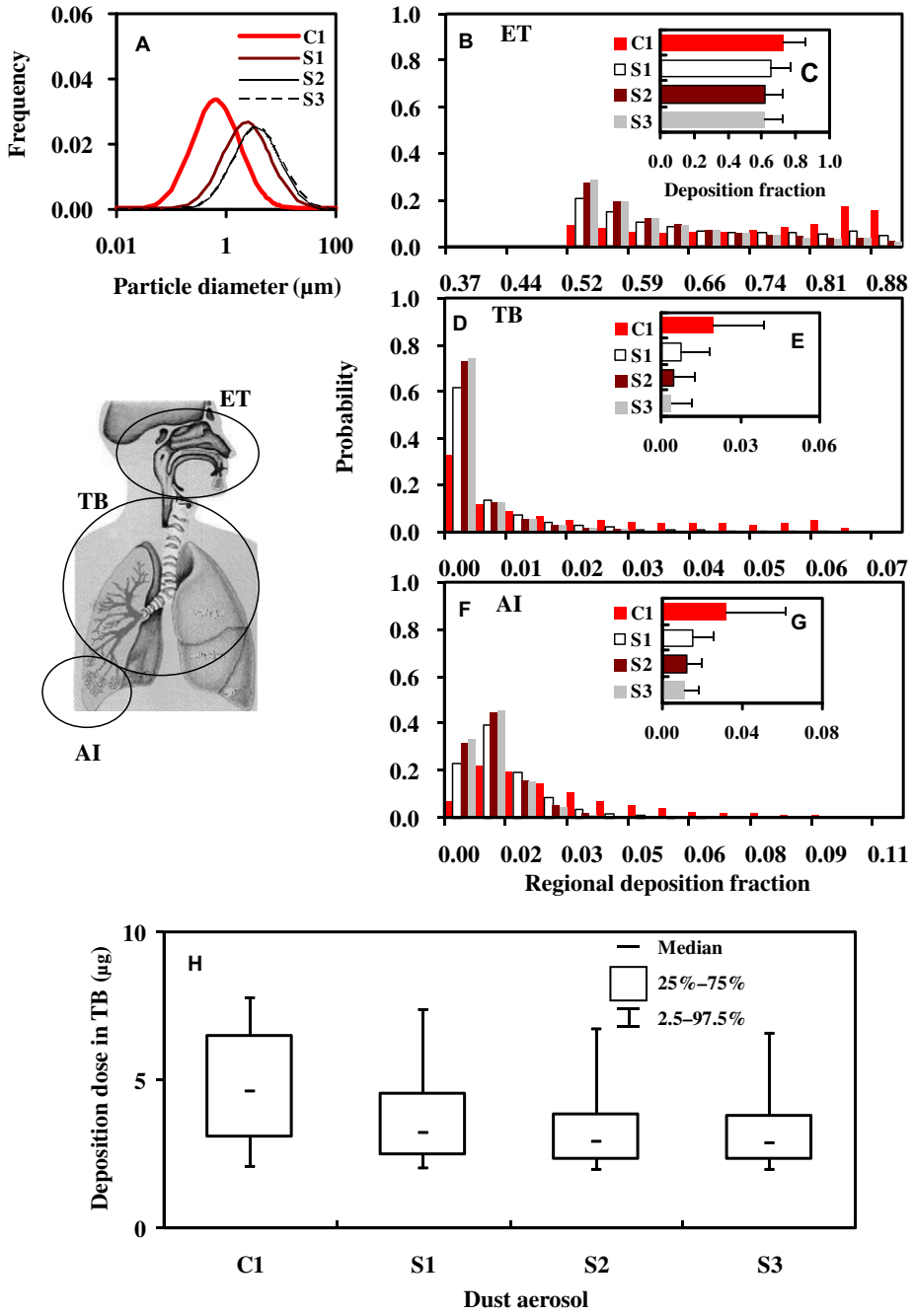

Fig. 2. (A) Reconstructed fraction of size distributions for airborne dust aerosols with clay (C1) and sand (S1, S2, S3) dusts. (B–G) Probability distribution of mass concentration-based regional deposition fraction and (H) the box-plots of deposition doses for challenge dust aerosols in TB region.

had the highest deposition fraction than TB and AI regions. The average deposition fractions with standard deviation in ET region were 0.73(0.13), 0.65(0.12), 0.62(0.11), 0.61(0.10) for C1, S1, S2, S3 dust aerosol (Fig. 2C). The deposition fractions in TB and AI regions were 0.019(0.019) and 0.032(0.030) for C1, 0.007(0.011) and 0.015(0.011) for S1, 0.005(0.008) and 0.012(0.007) for S2, and 0.004(0.007) and 0.011(0.007) for S3 dust, respectively (Fig. 2E, G). Among four types of aerosols, clay dust had higher probability for depositing larger amount doses in different respiratory regions. For clay dust, the average deposition fractions were 0.73, 0.02, and 0.03 in ET, TB, AI regions, respectively (Fig. 2C, E, G). Our results also revealed that the deposition dose for clay dusts in TB region (4.6 μg, 95% CI: 2.0–7.8 μg) was higher than the other sand dusts of 3.2 μg (2.5–7.4 μg), 2.9 μg (2.3–6.7 μg), and 2.9 μg (2.3–6.6 μg) for S1, S2, and S3, respectively (Fig. 2H).

To construct the aerosols binding kinetics-based TD model, the experimental aerosol challenge data were used to judge the model predictability. Fig. 3A–D shows the fitted time-course of %FEV_1 change with different size-specific dust aerosols, indicating the observed were consistent with predicted %FEV_1 decrements ($r^2 = 0.99$). To judge the model performance, the result showed that experimental observed and modeling predicted %FEV_1 decrements had better correlation ($r = 0.94$, $p < 0.001$) (Fig. 3E).

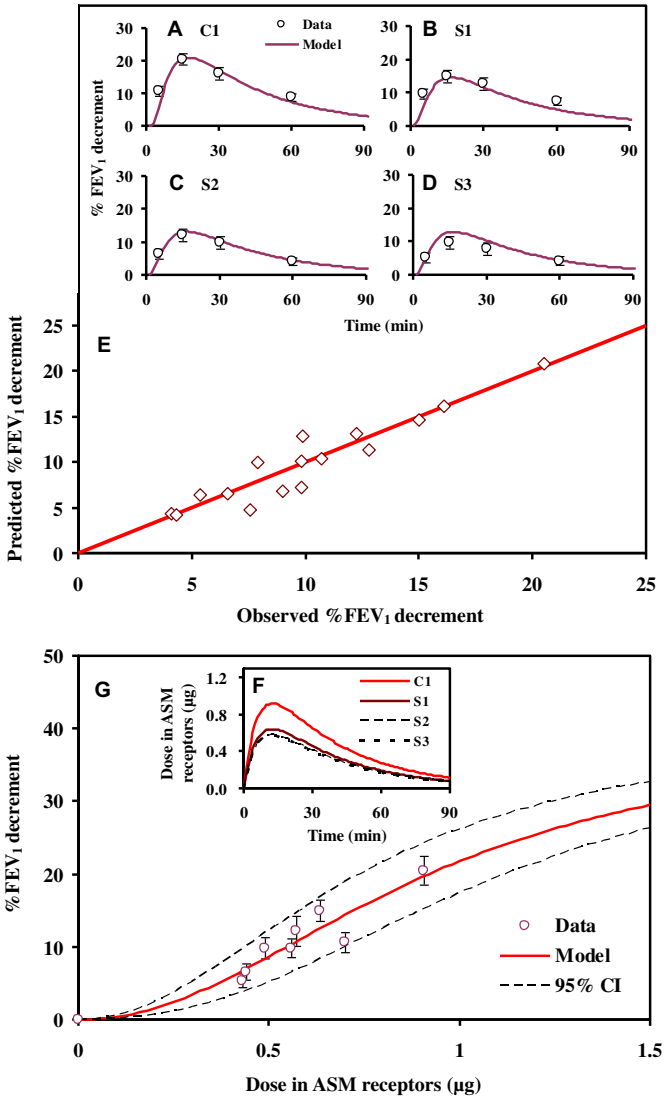

Fig. 3. (A–E) Calibration of model performance for the observation from the all data series ($N = 16$). The linear curve judges the well-predicted model performance. (F) Binding kinetics of binding dust aerosols in ASM receptors. (G) Reconstructed Hill model-based dose–response profiles for binding dust aerosols-induced %FEV_1 decrement.

Table 1 summarizes the initial conditions of the TK/TD model and the model parameter values used to estimate dust aerosols-associated lung function decrement. In model simulation processes, some parameter estimates were obtained via data fitting, whereas several available values were adopted from literature. The parameters for sensitization (λ_1) and desensitization (λ_2) rates of lung function were based on the fitted experimental aerosol challenge data in asthmatics which were estimated to be 9.51 μg^{-1} min^{-1} and 0.41 min^{-1}, respectively. Based on the TK/TD model with parameter values in Table 1, the binding kinetics of dust aerosol doses in ASM can be obtained (Fig. 3F). The ASM binding dose for four types of dust aerosol in the time-course of 15 and 30 min were incorporated into the asthmatic challenge results to construct dose–response relationships. The used time course of binding dose and %FEV_1 decrement can reveal the inflammatory and exacerbating process of airway directly.

The constructed Hill function-based dose–response profile was shown in Fig. 3G. The Hill model provides an adequate fit for the pooled data from binding dust aerosols in ASM receptors on %FEV_1 decrement ($r^2 = 0.93$). The result indicated that estimated median effective dose (ED50) for %FEV_1 decrement was 0.92 μg (95% CI: 0.74–1.09 μg) with the fitted Hill coefficient (n) of 2.1 (95% CI: 1.2–3.0), indicating that the situation of dust aerosols binding to ASM receptors was significant. In addition, all fitted coefficients in Hill model were judged significant ($p < 0.001$).

3.2. Exposure assessment

Table 2 summaries the collected monitoring data for PM_{10} and $PM_{2.5}$ concentration of dust storm aerosols from previous studies in Taipei, Taichung, and Pingtung situated in north, central, and south Taiwan regions, respectively. The MMD for ADS aerosols ranged from 1.03 to 3.19 μm which had smaller size distributions than challenge aerosols from Gupta et al. (2012). Based on the investigated data from Kuo and Shen (2010), we calculated the indoor/outdoor (I/O) ratio of nearly 0.4. In severe ADS events, the mean PM_{10} concentration can exceed 200 μg m^{-3} in three selected regions.

Fig. 4 shows the distributions of PM_{10} concentration and deposition dose of dust aerosols in setting scenarios. Based on the

Table 1
Point values of parameter values as well as initial values used in the TK/TD model.

Symbol	Meaning	Unit	Value			
			C1	S1	S2	S3
Variable						
$D_W(0)$	Initial PM dose in airway wall tissue	μg	4.58	3.19	2.89	2.85
$D_R(0)$	Initial PM dose in ASM cell receptor	μg	0			
$F(0)$	Baseline of %FEV_1 decrement		0			
Parameter						
k_b	Binding rate	min^{-1}	0.05[a]			
k_u	Unbinding rate	min^{-1}	0.1[a]			
c	Clearance rate	min^{-1}	0.05[a]			
λ_1	Sensitization rate	μg^{-1} min^{-1}	9.51[b]			
λ_2	Desensitization rate	min^{-1}	0.41[b]			

[a] Adopted from Amin et al. (2010).
[b] Estimated from observed data.

Table 2
Published data for PM concentration during dust storm periods in Taiwan.

Regions	Period	$PM_{2.5}$ ($\mu g\ m^{-3}$)	PM_{10} ($\mu g\ m^{-3}$)	MMD (μm)	Reference
North Taiwan					
Taipei city	Feb. 2002	34 ± 14[a]	116.4 ± 66.9	2.52	Lee et al. (2006)
	Mar. 2010	72.5 ± 55.4	432.8 ± 529.1	NA	TEPA
Central Taiwan					
Taichung city	Mar. 2001	56.6 ± 4.0	118.95 ± 12.6	3.19	Fang et al. (2002)
OD	Mar. 2004	75.73 ± 16.9[b]	118.55 ± 21.3	2.25	Kuo and Shen (2010)
ID	Mar. 2004	46.48 ± 20.3	47.03 ± 20.3	1.03	
	Mar. 2010	179 ± 59.4	326.7 ± 293.7	NA	TEPA
South Taiwan					
Pingtung city	Apr. 2001	70.2	156 ± 9.9	2.14	Chen et al. (2004)
	Mar. 2010	75.1 ± 49.7	284.6 ± 232.9	NA	TEPA

Abbreviations: TEPA = Taiwan Environmental Protection Agency; PM_{10} = Particulate matter with aerodynamic diameter less than 10 μm, $PM_{2.5}$ = Particulate matter with aerodynamic diameter less than 2.5 μm; MMD = Mass median diameter; OD = Outdoor; ID = Indoor; NA = Not available.
[a] Mean ± Standard deviation.

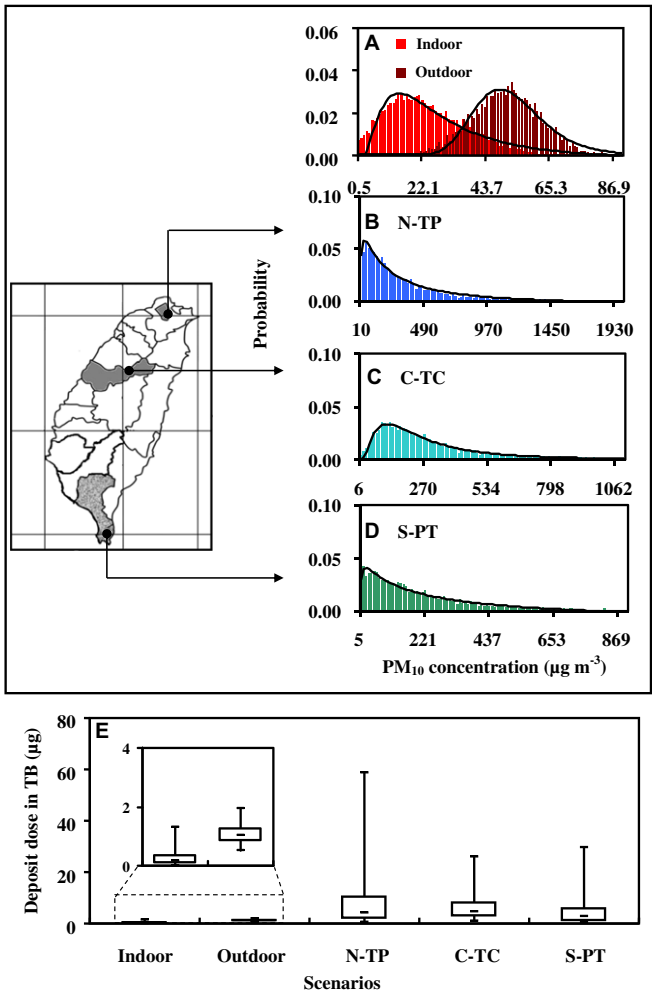

Fig. 4. (A–D) Exposure and (E) deposited dose distributions of dust aerosols in mild ADS events in indoor/outdoor setting and severe ADS events in Taipei (N-TP), Taichung (C-TC), and Pingtung (S-TP), respectively.

published data, the indoor setting had lower mass concentration distribution of LN(18.6 μg m^{-3}, 2.2) than outdoor setting LN(48.6 μg m^{-3}, 1.3) under mild dust storm events (Fig. 4A). However, there is the higher PM_{10} values measured in Taipei (N-TP) and Taichung (C-TC) than in Pingtung (S-PT) in outdoor setting. The concentration distributions of exposure were estimated to be LN(204 μg m^{-3}, 3.7), LN(218 μg m^{-3}, 2.4), and LN(128 μg m^{-3}, 3.3) in N-TP, C-TC, and S-PT, respectively (Fig. 4B, C, D). The results showed that gsd estimates of N-TP and S-PT were greater than that of C-TC, indicating that severe ADS in Taipei and Pingtung were caused the extreme high PM_{10} concentration in short time period. In Taichung, there were only slower concentration changes during the severe ADS period.

Fig. 4E shows the probability profiles for the predicted doses for the dust aerosols in TB region in mild I/O and severe city settings. The higher deposition dose distribution during severe ADS period can be estimated to be 4.27 μg (95% CI: 0.31–58.74 μg) in N-TP, 4.59 μg (95% CI: 0.78–25.9 μg) in C-TC, and 2.64 μg, (95% CI: 0.23–29.4 μg) in S-PT, respectively. During mild dust storm duration, the deposition dose distributions in I/O settings were 0.17 μg (95% CI: 0.02–1.30 μg) and 1.02 μg (95% CI: 0.52–1.95 μg), respectively (Fig. 4E).

3.3. Risk estimation

The risk estimates for $\%FEV_1$ decrement were based on the input scenario settings of ADS events in mild and severe burden distribution on ASM receptors. The simulated distributions of ASM binding aerosols were LN(0.03 μg, 2.9) and LN(0.21 μg, 1.4) in mild I/O settings, respectively (Fig. 5A). The risk curves for the dust aerosols-induced lung function decrement (Fig. 5B) indicated that the probabilities that 20% or more asthmatics (risk = 0.2) may decrease the $\%FEV_1$ approximately to 2.7% (95% CI: 1.3–4.1%) and 0.19% (0.08–0.31%) in I/O settings, respectively.

The simulated burden distribution of dust aerosols on ASM were LN(0.86 μg, 3.8), LN(0.92 μg, 2.4), and LN(0.52 μg, 3.4) in N-TP, C-TC, and S-PT, respectively, under the severe ADS events (Fig. 5C, E, G). Our results indicated that the risk = 0.5 of asthmatic in N-TP, C-TC, and S-PT may induce 16.9% (95% CI: 12.4–21.5%), 18.9% (14.3–23.4%), and 7.1% (4.0–10.2%) FEV_1 decrement, respectively, indicating that higher asthma exacerbation risk were occurred in north and central Taiwan (Fig. 5D, F, H).

3.4. Risk control efficiency

This study compared the inhaled dose of dust aerosols for no control and two surgical masks measures (Table 3). Table 3 indicates that 50th percentiles of inhaled dose for general mask in north, central, and south Taiwan were 0.88, 0.95, and 0.53 μg, respectively. The activated carbon of respirator protections can filtrate more dust aerosols which can reduce the inhaled dose to 0.16, 0.17, and 0.10 μg in northern, central, and southern Taiwan, respectively. Table 4 summaries the exceedance thresholds for the probabilities of $\%FEV_1$ decrement at risks of 0.8, 0.5, and 0.2 for asthmatics during the severe ADS period. The activated carbon of respirator protection had higher control efficiency for dust aerosols than general mask. In the 20th percentile of exceedance risk (ER = 0.2), activated carbon of respirator protections can reduce the inhaled dust aerosol dose and protect $\%FEV_1$ decrement up to less than 1%. The general mask only can control the $\%FEV_1$ decrement under 7.9% (95% CI: 4.6–11.2%), 5.4% (2.8–7.9%) and 3.3% (1.6–5.0%) in north, central, and south Taiwan, respectively. In addition, asthmatics will under high exacerbation risk when there have no control measure implemented in the severe ADS events.

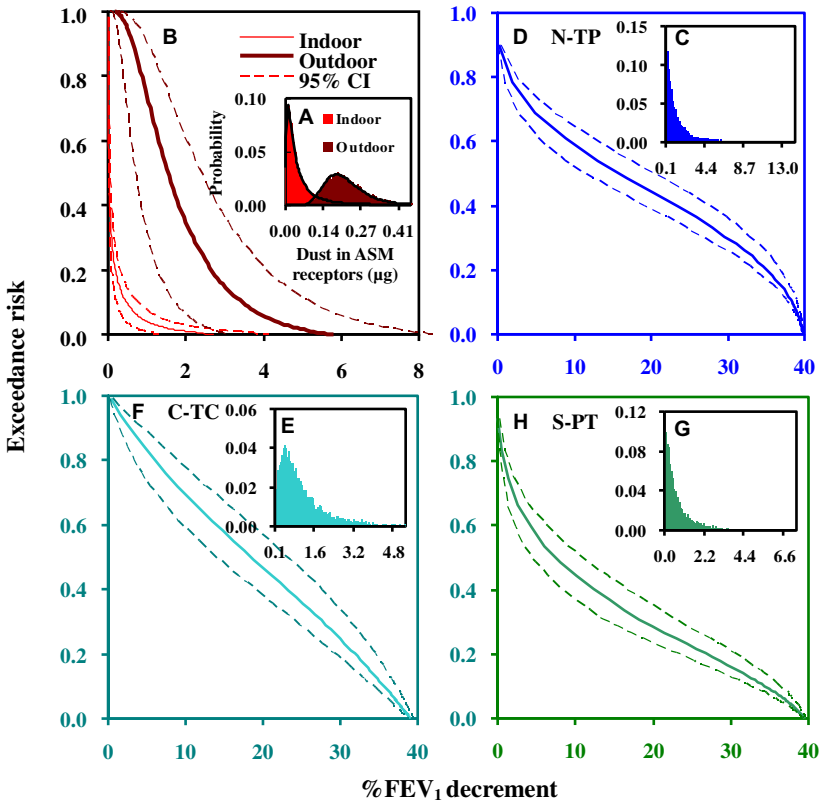

Fig. 5. Estimated exceedance risk curves with 95% CI of %FEV_1 decrement for asthmatics in mild indoor/outdoor setting (A, B) and severe dust storms events in Taipei (N-TP) (D, C), Taichung (C-TC) (F, E), and Pingtung (S-TP) (H, G), respectively, based on the input probability density functions of dust aerosols burden on ASM followed a log-normal distribution.

4. Discussion

4.1. Exposure and inhaled dose estimates

In this study, the empirical model from ICRP had given a valuable opportunity to quantify the inhaled dose for airborne dust. Gupta et al. (2012) found that dust aerosols with smaller size had greater potential to exacerbate airway function in asthmatic individuals. The inhaled doses for size-specific dust aerosols were difficult to detect. Based on our result, the smaller size of airborne dust had higher inhaled probability into deep lung regions TB and AI. In epidemiological studies, the asthma incidence was strongly associated with exposure to fine ($PM_{2.5}$) airborne particles (Green et al., 2000). The surfactant lower airway including TB and AI, are important region for maintaining small airway patency.

During Taiwan ADS events, particle size of airborne dust could as small as fine particle, indicating that dust aerosols sizes of MMD ranged from 1.03 to 3.19 μm (Lee et al., 2006). However, the exogenous triggers may induce the bronchial hyperactively and inflammation. These immune mechanisms would further induce constriction and obstruction in small airway (Green et al., 2000). Green et al. (2000) also found that deposition dose in region TB was

Table 3
Compare of different surgical masks to reduce the inhaled dose of dust aerosols.

Control measure	Deposition dose for various percentile (μg)				
	10	25	50	75	90
North Taiwan (N-TP)					
Without control	0.77	1.76	4.27	10.62	24.46
General mask	0.15	0.35	0.88	2.22	4.98
Activated carbon mask	0.03	0.06	0.16	0.40	0.93
Central Taiwan (C-TC)					
Without control	1.47	2.53	4.59	8.33	14.45
General mask	0.27	0.50	0.95	1.80	3.20
Activated carbon mask	0.04	0.08	0.17	0.33	0.57
South Taiwan (S-PT)					
Without control	0.54	1.12	2.64	6.05	12.71
General mask	0.10	0.22	0.53	1.31	2.90
Activated carbon mask	0.02	0.04	0.10	0.54	0.60

Table 4
Estimated lung function decrement at exceedance risks 0.2, 0.5, and 0.8 based on different control measures for site-specific dust storm events.

%FEV_1 decrement Setting	Exceedance risk		
	0.2	0.5	0.8
North Taiwan (N-TP)			
Without control	35.3 (33.6–36.9)[a]	16.9 (12.4–21.5)	1.8 (0.8–2.8)
General mask	7.9 (4.6–11.2)	0.8 (0.4–1.2)	0.05 (0.01–0.09)
Activated carbon mask	0.31 (0.13–0.49)	0.03 (0.01–0.05)	$<10^{-2}$
Central Taiwan (C-TC)			
Without control	32.2 (29.7–34.7)	18.9 (14.3–23.4)	6.0 (3.3–8.8)
General mask	5.4 (2.8–7.9)	1.2 (0.5–1.9)	0.22 (0.09–0.35)
Activated carbon mask	0.18 (0.08–0.28)	0.03 (0.01–0.05)	$<10^{-2}$
South Taiwan (S-PT)			
Without control	26.7 (23.0–30.4)	7.1 (4.0–10.2)	0.8 (0.4–1.2)
General mask	3.3 (1.6–5.0)	0.64 (0.56–0.72)	0.03 (0.01–0.04)
Activated carbon mask	0.11 (0.05–0.16)	$<10^{-2}$	$<10^{-2}$

[a] Median (95% CI).

lower for sand dust that might cause mild pulmonary response in asthmatics.

Due to the ASM is the major tissue in response to environmental stimuli, this study used deposition dust aerosols in airways as reactive dose to construct the TK/TD model-based dose–response relationship. Amin et al. (2010) introduced the PK model to predict agonist-receptors binding kinetic between ASM receptors and walls. The PK model was primary used to simulate the dynamic pressure-driven breathing in lung airways which can consider the different settings of tissue properties, flow dynamics, and agonist doses. They further indicated that the changes of airway constriction were dependent on the burden of ASM binding dose.

The exogenous airway stimulation will cause the heterogeneous bronchoconstriction in lung ventilation (Venegas et al., 2005). The clearance rate of deposited particle is the key parameter which can determine the lung function exacerbation. Möller et al. (2006) indicated that individuals with pulmonary disorder may cause the longer retention time of inhaled particles than healthy subjects which may cause the severity of pulmonary disease. In addition, the physical properties also affect the clearance time such as solubility and size of particles (Asgharian et al., 2001). However, the developed TK/TD model cannot predict the proportions of airway constriction in respiratory tract. The ventilation of lung airways was assumed to be in the homogeneous conditions. Due to the sources of reference value are rare, the parameters of lung mechanics for sensitization and desensitization rates of FEV_1 can only be estimated from experimental data in the TD modeling.

4.2. Quantification of risk and control strategy

Our results could further understand the causing factor for disease exacerbation for asthmatic exposed to size-specific PM during dust storm events. The disease patient used FEV_1 as reliable indicator to reflect health status of airway function in aerosol challenge. In addition, previous study also used PEF of lung function to detect asthma exacerbation during the ADS period (Hong et al., 2010). We found that the indoor staying would lower the exposure level and provide health protection during the ADS period. In western Japan, Watanabe et al. (2011) found that ADS can increase aggravated lower respiratory symptoms such as cough and sputum in adult asthma, but the influence was slightly. Furthermore, not only among adult populations, the school children also could suffer from the ADS attack (Hong et al., 2010).

Under the severe ADS event, this study found that there were 50% probability of decreasing $\%FEV_1$ exceed 16.9, 18.9, and 7.1% in north, center, and south Taiwan, respectively. To control the health effect during the ADS period, the control strategy of mask wearing can provide the effective protection for reducing the inhaled dust aerosols. In this study, the use of the activated carbon of mask respirators had the best efficiency for reducing the inhaled dust aerosol dose, by which the $\%FEV_1$ decrement can be reduced up to less than 1%. Recent study also demonstrated that the face masks may effectively reduce individuals' particulate matters exposure and reduce health risks (Langrish et al., 2012). The only limitation is to know whether efficiency would be sustained with face-mask use over a longer period.

4.3. Limitation and implication

Our study provides the mechanistic models to quantify the effects of ADS events on lung function decrement in asthmatics. There are some limitations in our analyses. We used ASM binding aerosols as effective dose and assumed that TB region is an important part to reflect airway disorder. Although there is possibility for aerosols deposited in ET and AI regions that may cause lung function decrement, this study only considered the appropriate assumptions to construct the dose–response relationships. In addition, many studies have indicated that number concentration is the important quantitative unit in the toxicological experiments. This study found that mass concentration had better correlation than number concentration with lung function effect in dose–response construction. Therefore, we used mass concentration to estimate the inhaled dose of dust aerosol.

In exposure analysis, there were no available size distribution data from monitoring stations. This study integrated the size distribution from previous studies to simulate the probable size distribution in severe ADS events due to the similar physical properties for ADS aerosols. The size distribution can further be used to calculate the size-dependent deposition fraction of dust aerosols in severe ADS event.

There are uncertainties in assessing the PM-associated respiratory health. Penttinen et al. (2001) found that the number concentration of accumulation $PM_{2.5}$ was inversely but non-significantly associated with PEF of lung function for adult asthmatics. Trenga et al. (2006) found that pediatric asthmatics are the susceptible population that can cause severe lung function effects under particulate air pollution exposure. However, the adult lung function cannot be associated with $PM_{2.5}$ concentration. Although there are multiple variables to assess the PM-associated respiratory health, it is difficult to adjust the age-specific lung function effect during ADS periods.

Previous studies indicated that ADS events were associated with hospital admission such as asthma, pneumonia, and cardiovascular disease (Chan et al., 2008). Yang et al. (2005) indicated that insignificant relationships were found between ADS events and daily admissions for asthma in Taipei, Taiwan in the period 1996–2001. They claimed that the dust storm days can only increase the risk of asthma admissions slightly. On the other hand, Bell et al. (2008) found that ADS events and PM_{10} concentrations can significantly increase the risk of asthma hospitalization in Taipei in the period 1995–2002. However, some potential challenges still exist for implementing our study in the real situations.

Dust aerosols exposure may also induce other cardiovascular diseases. Chang et al. (2007) designed an exposure protocol to investigate the physical changes in spontaneously hypertensive rats during the ADS events exposure in Taiwan. The result found that ADS particles can cause alterations of heart rate, blood pressure, and cardiac contractility. Moreover, the epidemiological studies also found that ADS increased mortality in Taiwan (Chen et al., 2004; Chan and Ng, 2011). In this study, we only focus on the risk for ADS events-induced lung function decrement. We can further assess the mortality risk due to dust aerosols exposure by the mechanistic models.

To assess the exposure risk of ADS aerosols, this study used the total mass concentration of dust aerosols to calculate effective dose. Some studies indicated that the metal concentrations bound to the particulates were the major trigger for causing lung disease exacerbation. Higher concentrations of metal elements such as Al, Fe, Mg, and Ca-rich particles in $PM_{2.5-10}$ were measured during the ADS events in Taiwan (Cheng et al., 2005). Hong et al. (2010) indicates that children's pulmonary function may reduce due to exposure to the metals bound to particles during the ADS period. The metal concentrations of the PM were associated with asthma attack. Recently, no toxicological experiment provides the relationship between component concentration in dust aerosols and lung function exacerbation for asthmatics. Therefore, we cannot use the component of metal and organic elements which may cause the different levels of respiratory effect. In future research, we would focus on the specific component which is the major trigger for causing lung disease exacerbations.

5. Conclusions

We constructed the human health risk assessment protocol to assess dust storm events-associated lung function decrement. The developed TK/TD model helps us for better understanding the inhaled aerosol dose-associated airway function changes. We concluded that Taiwan ADS events pose potential threat to exacerbate CRDs and could cause lung function decrement. Our result implicates that the use of activated carbon of mask respirators has the best efficacy for reducing inhaled dust aerosol dose. Further theoretical and experimental analyses are required to achieve a better understanding of ADS-induced CRDs exacerbation risk. There were rooms for further improvements, especially in better understanding the experimental ADS exposure of respiratory symptoms and the effect of dust aerosols on lung function in asthmatics.

References

Amin, S.D., Mahumdar, A., Frey, U., Suki, B., 2010. Modeling dynamics of airway constriction: effects of agonist transport and binding. Journal of Applied Physiology 109, 553–563.

Asgharian, B., Hofmann, W., Miller, F.J., 2001. Mucociliary clearance of insoluble particles from the tracheobronchial airways of the human lung. Journal of Aerosol Science 32, 817–832.

Bell, M.L., Levy, J.K., Lin, Z., 2008. The effect of sandstorms and air pollution on cause-specific hospital admissions in Taipei, Taiwan. Occupational Environmental Medicine 65, 104–111.

Chan, C.C., Chuang, K.J., Chen, W.J., Chang, W.T., Lee, C.T., Peng, C.M., 2008. Increasing cardiopulmonary emergency visits by long-range transported Asian dust storms in Taiwan. Environmental Research 106, 393–400.

Chan, C.C., Ng, H.C., 2011. A case-crossover analysis of Asian dust storms and mortality in the downwind areas using 14-year data in Taipei. Science of the Total Environment 410–411, 47–52.

Chang, C.C., Hwang, J.S., Chan, C.C., Wang, P.Y., Cheng, T.J., 2007. Effects of concentrated ambient particles on heart rate, blood pressure, and cardiac contractility in spontaneously hypertensive rats during a dust storm event. Inhalation Toxicology 19, 973–978.

Chen, C.H., Xirasagar, S., Lin, H.C., 2006. Seasonality in adult asthma admissions, air pollutant levels, and climate: a population-based study. Journal of Asthma 43, 287–292.

Chen, C.W., 2001. Evaluation of Filter Performance. Report No. IOSH89-H308 (in Chinese).

Chen, Y.S., Sheen, P.C., Chen, E.R., Liu, Y.K., Wu, T.N., Yang, C.Y., 2004. Effects of Asian dust storm events on daily mortality in Taipei, Taiwan. Environmental Research 95, 151–155.

Cheng, M.T., Lin, Y.C., Chio, C.P., Wang, C.F., Kuo, C.Y., 2005. Characteristics of aerosols collected in central Taiwan during an Asian dust event in spring 2000. Chemosphere 61, 1439–1450.

Department of Health (DOH), 2007. Compilation of Exposure Factors. Report No. DOH96-HP-1801. (in Chinese).

Fang, G.C., Chang, C.N., Wu, Y.S., Lu, S.C., Fu, P.P.C., Chang, S.C., Cheng, C.D., Yuen, W.H., 2002. Concentration of atmospheric particulates during a dust storm period in central Taiwan, Taichung. Science of the Total Environment 287, 141–145.

Freijer, J.I., van Eijkeren, J.C.H., van Bree, L., 2002. A model for the effect on health of repeated exposure to ozone. Environmental Modeling and Software 17, 553–562.

Frey, U., Maksym, G., Suki, B., 2011. Temporal complexity in clinical manifestations of lung disease. Journal of Applied Physiology 110, 1723–1731.

Global Initiative for Asthma (GINA), 2012. Available from: http://www.ginasthma.com.

Green, F.H.Y., Schurch, S., Lee, M., Gehr, P., 2000. The role of surfactant in disease associated with particle exposure. In: Gehr, P., Heyder, J. (Eds.), Particle-Lung Interactions. Macel Dekker, New York, pp. 533–576.

Gupta, P., Singh, S., Kumar, S., Choudhary, M., Singh, V., 2012. Effects of dust aerosol in patients with asthma. Journal of Asthma 49, 134–138.

Hinds, W.C., 1999. Aerosol Technology: Properties, Behavior and Measurement of Airborne Particles, second ed. John Wiley & Sons Inc, New York.

Hong, Y.C., Pan, X.C., Kim, S.Y., Park, K., Park, E.J., Jin, X., et al., 2010. Asian dust storm and pulmonary function of school children in Seoul. Science of the Total Environment 408, 754–759.

ICRP, 1994. Human Respiratory Tract Model for Radiological Protection, a Report of a Task Group of the International Commission on Radiological Protection. ICRP Publication No. 66. Pergamon Press, New York.

Kuo, H.W., Shen, H.Y., 2010. Indoor and outdoor $PM_{2.5}$ and PM_{10} concentrations in the air during a dust storm. Building and Environment 45, 610–614.

Langrish, J.P., Li, X., Wang, S., Lee, M.M., Miller, M.R., Cassee, F.R., et al., 2012. Reducing personal exposure to particulate air pollution improves cardiovascular health in patients with coronary heart disease. Environmental Health Perspectives 120 (3), 367–372.

Lee, C.T., Chuang, M.T., Chan, C.C., Cheng, T.J., Huang, S.L., 2006. Aerosol characteristics from the Taiwan aerosol supersite in the Asian yellow-dust periods of 2002. Atmospheric Environment 40, 3409–3418.

Lee, Y.L., Lin, Y.C., Hsiue, T.R., Hwang, B.F., Guo, Y.L.L., 2003. Indoor and outdoor environmental exposures, parental atopy, and physician-diagnosed asthma in Taiwanese schoolchildren. Pediatrics 112, E389–E395.

Liu, C.M., Young, C.Y., Lee, Y.C., 2006. Influence of Asian dust storms on air quality in Taiwan. Science of the Total Environment 368, 884–897.

Möller, W., Häußinger, K., Ziegler-Heitbrock, L., Heyder, 2006. Mucociliary and long-term particle clearance in airways of patients with immotile cilia. Respiratory Research 7, 10.

Nel, A., 2005. Air pollution-related illness: effects of particles. Science 308, 804–806.

Penttinen, P., Timonen, K.L., Tiittanen, P., Mirme, A., Ruuskanen, J., Pekkanen, J., 2001. Number concentration and size of particles in urban air: effects on spirometric lung function in adult asthmatic subjects. Environmental Health Perspectives 109, 319–323.

Pope, C.A., Dockery, D.W., 2006. Health effects of fine particulate air pollution: lines that connect. Journal of the Air & Waste Management Association 56, 709–742.

Ruzer, L.S., Harley, N.H., 2005. Aerosols Handbook: Measurement, Dosimetry, and Health Effects. CRC Press, New York.

Taiwan Environmental Protection Administration, Executive Yuan. Available at: <http://www.epa.gov.tw>.

Trenga, C.A., Sullivan, J.H., Schildcrout, J.S., Shepherd, K.P., Shapiro, G.G., Liu, L.J., et al., 2006. Effect of particulate air pollution on lung function in adult and pediatric subjects in a Seattle panel study. Chest 129, 1614–1622.

Tsai, S.S., Cheng, M.H., Chiu, H.F., Wu, T.N., Yang, C.Y., 2006. Air pollution and hospital admissions for asthma in a tropical city, Kaohsiung, Taiwan. Inhalation Toxicology 18, 549–554.

Venegas, J.G., Winkler, T., Musch, G., Melo, M.F.V., Layfield, D., Thavalekos, N., et al., 2005. Self-organized patchiness in asthma as a prelude to catastrophic shifts. Nature 434, 777–782.

Watanabe, M., Yamasaki, A., Burioka, N., Kural, J., Yoneda, K., et al., 2011. Correlation between Asian dust storms and worsening asthma in western Japan. Allergology International 60, 267–275.

Weiss, S.T., 2010. Lung function and airway diseases. Nature Genetics 42, 14–16.

Yang, C.Y., Tsai, S.S., Chang, C.C., Ho, S.C., 2005. Effects of Asian dust storm events on daily admissions for asthma in Taipei, Taiwan. Inhalation Toxicology 17, 817–821.